RSC Advances

PAPER

View Article Online
View Journal | View Issue

Cite this: *RSC Adv.*, 2015, **5**, 1343

Direct growth of etch pit-free GaN crystals on few-layer graphene†

Seung Jin Chae,[ab] Yong Hwan Kim,[ab] Tae Hoon Seo,[c] Dinh Loc Duong,[ab] Seung Mi Lee,[d] Min Ho Park,[e] Eun Sung Kim,[ab] Jung Jun Bae,[ab] Si Young Lee,[ab] Hyun Jeong,[a] Eun-Kyung Suh,[c] Cheol Woong Yang,[e] Mun Seok Jeong*[ab] and Young Hee Lee*[ab]

Received 17th October 2014
Accepted 27th November 2014

DOI: 10.1039/c4ra12557f

www.rsc.org/advances

We report high-quality GaN crystals grown directly on graphene layers without a buffer layer by metal–organic chemical vapour deposition. Photoluminescence and Raman spectra revealed that GaN crystals grown on graphene layers had mild strain as compared to those grown on sapphire and SiO_2 substrates. Etch pits were not observed on the surface of GaN/graphene, in which threading dislocations were diminished inside the bulk. This is markedly different from GaN/sapphire, in which threading dislocations were present on GaN surfaces. This opens a new possibility that graphene with π electrons and hexagonal symmetry could be an ideal substrate for GaN crystal growth instead of expensive sapphire substrates.

Introduction

Group III nitrides of inorganic compound semiconductors are widely used for light-emitting diodes and high-power/high-frequency electronic devices.[1,2] Control of GaN crystal quality with a minimum threading dislocation density (TD) is a key step to realizing such devices.[3–5] Sapphire is the most commonly used substrate, but the mismatch of crystal lattices and thermal expansion coefficients between GaN and the sapphire substrate causes dislocations on the growing GaN. Developing a new type of substrate with low cost and easy handling is highly required.

Graphene is a layered structure of hexagonally arranged carbon atoms with strong σ bonds within the plane, whereas weak π electrons are exposed to the surface. Thus, the interaction of graphene with other materials is generally weak. For example, if GaN is grown on a graphene substrate, the lattice mismatch may be very different from that of GaN grown on sapphire, which may reduce the dislocation density or generate different types of dislocations. Ideally, the strain energy could be reduced owing to the weak interaction between graphene and the host material. Therefore, graphene could act as an ideal substrate for the crystal growth of numerous materials.[6–10] In this report, we demonstrate this concept by introducing graphene as a substrate for direct growth of GaN instead of sapphire. Highly crystalline GaN (0001) on a graphene substrate was synthesized by metal–organic chemical vapour deposition (MOCVD) without using a buffer layer. No yellow band in the photoluminescence (PL) spectra was observed. Tensile stress accumulated on the GaN/graphene, but its magnitude was smaller than that of GaN/sapphire. Unlike GaN/sapphire, which shows threading dislocations on the GaN surface, etch pits were not observed on the surface of the GaN/graphene, where the threading dislocations were diminished inside the bulk material.

Results and discussion

Fig. 1 shows the field emission scanning electron microscope (FESEM) images with related schematics of GaN crystal growth on graphene. The pristine graphene on SiO_2 (300 nm)/Si (Fig. 1a), which was transferred from chemical vapour deposition (CVD)-grown graphene on a Ni substrate, shows typical wrinkles and bumpy structures. The white arrows indicate wrinkles, which are generated by differences in the thermal expansion coefficients of the Ni substrate and the graphene layers caused by thermal quenching during CVD.[11] The black arrows show bumpy structures, which are formed during the etching and transfer process on SiO_2/Si substrates.[12] The inset image indicates a few layers of graphene transferred onto the polyethylene terephthalate (PET, 4 × 3.5 cm) film. This

[a]Center for Integrated Nanostructure Physics, Institute for Basic Science, Sungkyunkwan University, Suwon 440-746, Republic of Korea. E-mail: leeyoung@skku.edu; mjeong@skku.edu

[b]Department of Energy Science, Department of Physics, Sungkyunkwan University, Suwon 440-746, Republic of Korea

[c]School of Semiconductor and Chemical Engineering, Chonbuk National University, Jeonju 561-756, Republic of Korea

[d]Center for Nanocharacterization, Korea Research Institute of Standards and Science, Daejeon 305-340, Korea

[e]Department of Advanced Materials Engineering, Sungkyunkwan University, Suwon 440-746, Korea

† Electronic supplementary information (ESI) available. See DOI: 10.1039/c4ra12557f

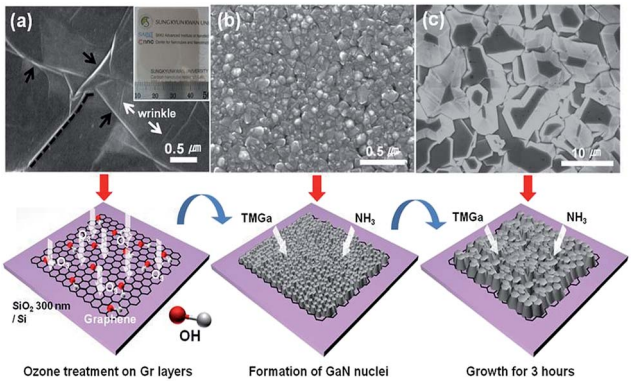

Fig. 1 FESEM images and corresponding schematics of GaN crystal growth on graphene. (a) As-synthesized graphene surface. White arrows indicate wrinkles. Black arrows indicate bumpy structures that formed during the graphene transfer process. The inset shows the transferred graphene on PET film (4 × 3.5 cm) with a transmittance of 80% at 550 nm. (b) Formation of initial nucleation seeds grown at 530 °C for 5 min. (c) GaN crystals grown at 1040 °C for 3 h following an initial nucleation step.

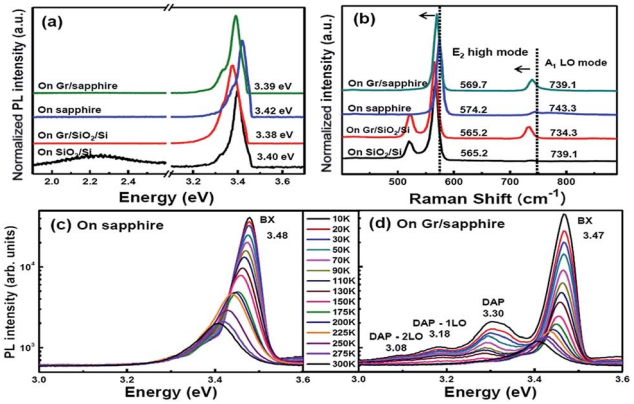

Fig. 2 (a) PL spectra from GaN crystals grown on sapphire, graphene, and SiO_2 substrates at a temperature of 300 K. A diode-pumped solid-state (DPSS) laser with a 355 nm wavelength was used as the excitation light. (b) Raman spectra from GaN samples grown on four types of substrates (Gr/sapphire, sapphire, Gr/SiO_2/Si, and SiO_2/Si) with an excitation wavelength of 532 nm. The dashed line shows the red-shift of the GaN crystal on graphene substrate. (c) and (d) Temperature-dependent GaN PL spectra from 10 K to 300 K on the sapphire and graphene substrates, respectively. The excitation wavelength was 325 nm. PL emission lines are labeled "BX" and "DAP" which represent luminescence from bound exciton and donor acceptor pair, respectively.

transferred graphene film has a transmittance of 80% at 550 nm or equivalently ~10 layers of graphene. The small D/G intensity ratio in the pristine graphene indicates the high quality of the grown graphene (see the ESI, Fig. S1†). After ozone treatment in the atomic layer deposition (ALD) chamber, the D-band intensity increased significantly. Oxygen functional groups such as epoxy and/or hydroxyl groups were likely formed owing to abundant defective sites in the CVD-grown graphene, as shown in the schematic of Fig. 1a. These sites may act as nucleation seeds for direct GaN growth. A two-temperature scheme was introduced to enhance the number of nucleation seeds for GaN grown directly on graphene: a low temperature of 530 °C for 5 min was used to form nucleation seeds and a high temperature of 1040 °C for 3 h was used for further growth. This approach is in contrast to a previous report in which a ZnO layer was used as a buffer layer prior to GaN growth.[13] Small agglomerates of GaN with sizes less than 100 nm were formed at the early low-temperature regime (Fig. 1b). The number of GaN nucleation seeds generated depended on the nucleation times (ESI, Fig. S2†). The wrinkles and bumpy structures on graphene also acted as nucleation seeds. With further growth at high temperature, GaN crystallites were formed with lateral sizes of several tens of micrometres and a height of 10 μm (Fig. 1c). Well-developed facets with various orientations were also visible from each crystallite, where the (0001) growth direction was retained from each crystallite.

Fig. 2a shows the photoluminescence (PL) spectra at room temperature of the grown GaN samples. GaN grown on the graphene (Gr)/SiO_2/Si and Gr/sapphire substrates showed clear excitonic PL peaks at 3.38 and 3.39 eV, respectively, without a yellow luminescence band. This is similar to the GaN grown on sapphire except for a slight peak shift from 3.42 eV, but it is in contrast with GaN grown on the SiO_2/Si substrate, in which a yellow luminescence (YL) band was observed at approximately 2.2 eV (band width ~1 eV), representing defect formation in the GaN film. The values for the full width at half maximum of the excitonic PL peaks for the three substrates were similar to each other, indicating that GaN crystallites grown on graphene have a crystal quality similar to that of GaN grown on sapphire. The respective red shifts of 0.03 and 0.04 eV for the GaN grown on the Gr/SiO_2/Si and Gr/sapphire substrates as compared to GaN grown on sapphire could be related to strain relaxation, which will be discussed later.

The presence of residual stress of the GaN film is well represented by the frequency shift and width of the E_2 high (E_2^H) mode.[14–18] Fig. 2b shows clear E_2^H and A1 LO modes for the four samples at room temperature. The E_2^H mode of strain-free GaN is 567 cm^{-1} (see Table 1). The GaN film grown on the sapphire substrate induces general compressive strain, whereas the GaN film on the silicon substrate induces tensile strain.[19] In Fig. 2b, the blue shift of the E_2^H peak frequency by 7.2 cm^{-1} for the GaN directly grown on sapphire and by 2.7 cm^{-1} for the GaN grown on the Gr/sapphire substrate corresponds to compressive strain, although the latter is milder than the former. This indicates that the strain is minimized by using graphene as a substrate. On the other hand, the red shift by 1.8 cm^{-1} in the GaN grown on the Gr/SiO_2/Si and SiO_2/Si substrates is an indication of mild tensile stress. This implies that the graphene transferred onto different substrates is slightly influenced by the substrate type, presumably owing to the surface morphology of the substrate.

Fig. 2c and d show the PL spectra of GaN on sapphire and on Gr/sapphire as a function of temperature from 10 K to 300 K. The spectra are dominated by neutral donor–bound recombination.[20] Red shifts and broadening of all emission lines were observed as the temperature decreased. The temperature

Table 1 The grown GaN relationships of substrate/equipment/Raman (E_2^H)/PL/thickness/TD density/stress/nucleation layer

	Substrate	Equip.	Raman (E_2^H)	PL (eV)	Thickness (μm)	Threading dislocation density (cm^{-2})	Stress	Nucleation layer
Ref. 14	—	HVPE	567		50	3×10^6	—	—
Ref. 15	Sapphire	HVPE	569.1	3.42	80	$<10^8$	—	—
Ref. 16	Si (111)	MOCVD	565.2	3.405	1.5, 2.5 (ref. 24)	-10^8 (ref. 24)	Tensile	Gan/AIN
Ref. 17	6H–SiC	MBE	565.3	3.414	2–5	4×10^8 (ref. 21)	Tensile	AIN
Ref. 18	Sapphire	MOCVD	568.5	3.432	2–5	—	Compressive	—
This work	Graphene/SiO_2/Si	MOCVD	565.2	3.38	10	$\frac{\text{Total dislocations density } (cm^{-2})}{7.6 \times 10^9}$	Tensile	GaN

dependence of the line width is attributed to phonon-induced band broadening.[21] The characteristic red shift with increasing temperature is attributed to band gap reduction from lattice expansion and to electron–phonon interaction.[22] As shown in Fig. 2c, no donor–acceptor pairs (DAP) were observed in GaN grown on sapphire. On the other hand, DAP lines were clearly visible in the GaN grown on Gr/sapphire. As shown in Table 2, the gaps between DAP, DAP-1LO, and DAP-2LO are nearly regulated with an interval of ~100 meV in the GaN grown on Gr/sapphire. Carbon could be a source of acceptor sites owing to the presumably disassembled graphene layers during nucleation of GaN by pyrolysis at high growth temperatures. Carbon doping in GaN crystals is generally obtained by implantation or by using CBr_4 gas.[23,24] In these methods, defects in GaN crystals are generated by physical force and etching, resulting in the appearance of a YL band. In the current case of Gr/sapphire, the carbon atoms were doped naturally by pyrolysis, without creating defect sites by physical damage.

The mild tensile stress in GaN grown on Gr/SiO_2/Si is markedly different from the high compressive stress accumulated in GaN grown on Gr/sapphire. Fig. 3 shows the theoretical simulation data based on density functional theory, which is generally used in nanostructure calculations.[25] Fig. 3a shows the ball-and-stick atomic structure of the GaN monolayer. The Ga–Ga or N–N distance is 3.18 Å. This closely matches the separation distance (3.23 Å) of the next bond-centre site of graphene, as shown in Fig. 3b. Every Ga and N atom is positioned at the bond-centre site of graphene. Overlapping a super cell of GaN on the graphene layer resulted in an alternative location of N atoms at every other top site of graphene (indicated by green dashed line) and Ga atoms alternatively at H (hexagonal) sites and bond-centre sites of graphene (red dashed line) (see Fig. 3c). As the number of Ga and N atoms increases to form a monolayer, the GaN structure is converted into a hexagonal phase. The Ga–N bond length approaches that of the bulk material, as shown in Fig. 3d, as the number of layers increases. Maintaining hexagonal symmetry and minimum strain as compared to hexagonal GaN/sapphire is an advantage of using graphene as a substrate. The graphene layer could be strained by the substrate, which is evidenced by the difference in the binding energy with and without relaxation of the graphene layer. On the other hand, the interfacial binding energy increases, becoming saturated to less than −3.0 eV per GaN at six GaN layers. This is the origin of stress of the grown GaN, even with a graphene substrate. At high growth temperatures,

Table 2 Comparison of DAP according to various dopant concentrations and temperatures

Dopant concentration (cm^{-3})	Temperature (K)	PL (eV): donor–acceptor pair (DAP)
Mg[36]: ~10^{17}	4	DAP: 3.26 DAP-1LO: 3.17
Be[37]: ~10^{18}	5	DAP: 3.38 DAP-1LO: 3.29 DAP-2LO: 3.20
Si[38]: ~10^{17}	2	DAP: 3.27 DAP-1LO: 3.18
C[39]: ~10^{18}	2	DAP: 3.15
This work	10	DAP: 3.30 DAP-1LO: 3.18 DAP-2LO: 3.08

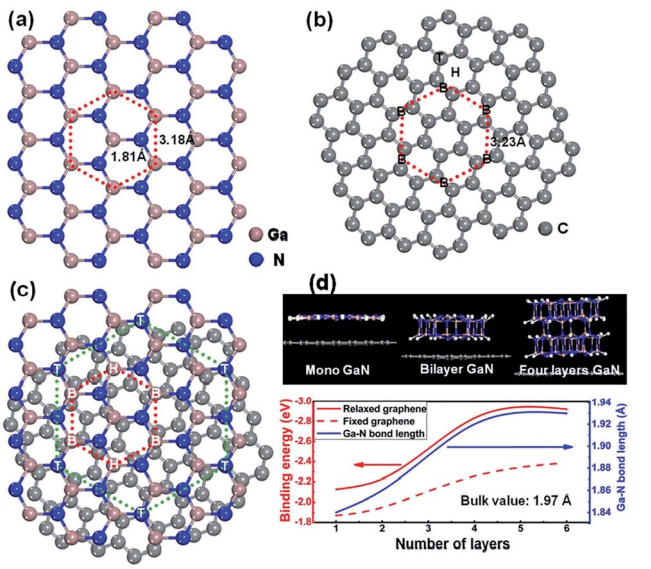

Fig. 3 (a) Lattice constants of GaN and (b) graphene super cell are 3.18 Å and 3.23 Å, respectively (B: bridge site, H: hexagonal site, T: top site). (c) Overlapped super cell structure of (a) and (b) indicate Ga-polar GaN grown on graphene. (d) Binding energy of GaN pair on graphene.

therefore, the grown GaN layers, in particular those near the interface, are expected to be slightly strained. Nevertheless, this interfacial energy is smaller than that of GaN/sapphire, as shown in the calculated strain, stress, and frequency shift in Table 3. As a consequence, we expect the strain developed on the graphene surface to be presumably smaller that on sapphire from the theoretical simulation data.

As shown in Table 3, using the phonon frequency (E_2^H) change with respect to the bulk value (567 cm^{-1}),[14] $\Delta\omega$ (cm^{-1}) = $C\sigma_{xx}$ formula,[26] already well known relationship to calculate the strain of GaN grown on sapphire and that of GaN grown on Gr/sapphire simultaneously, the biaxial stress (σ_{xx}) was extracted. The linear stress coefficient, C, is a constant value. Young's modulus ($E = \sigma/\varepsilon$) was used to obtain the strain value by substituting the value of the obtained stress. The mild tensile stress on GaN/Gr/SiO_2/Si was expected owing to the weak interaction between graphene and GaN. The strain of GaN/Gr/sapphire is approximately three times smaller than that of GaN/sapphire, as expected from the theoretical arguments given in the previous paragraph.

Fig. 4a shows the cross-sectional transmission electron microscope (TEM) images of GaN near the interface of graphene. The inset image clearly shows no defects such as voids or cracks. Multilayer (~10 layers) graphene with slight variations in thickness, which is a characteristic of multilayer graphene on a Ni substrate,[11] was also clearly visible at the interface. In addition, the high-resolution TEM image of GaN crystals in Fig. 4b indicates a well-aligned crystal lattice array. The lattice spacing between the nearby planes is 0.52 nm, in good agreement with the d-spacing of GaN (0001) planes grown on sapphire.[13] The electron diffraction pattern shows a (11$\bar{2}$0) zone axis pattern of the grown GaN crystal on graphene in Fig. 4c (see also ESI, Fig. S3†).

GaN epitaxial layers can be grown, in general, by the well-known two-step MOCVD method on (0001) sapphire.[27] These layers contain a high density of threading dislocations (TDs). There are three types of TDs in GaN: pure edge, pure screw, and mixed types. Epitaxial layers predominantly contain pure edge-type TDs that have a line direction perpendicular to the GaN sapphire interface. As a consequence, edge TDs are generated as a result of the large lattice mismatch between GaN and sapphire. TDs are detrimental to electronic and photoelectronic devices. The TD density is, therefore, a critical parameter for judging the quality of GaN films. To understand the formation of TDs in GaN grown on Gr/SiO_2/Si, we inspected two TEM cross-sectional micrographs. It is commonly presumed that TDs evolve from the coalescence of tilted and twisted islands during the initial stages of GaN deposition.[28] Bright-field TEM images, recorded under two-beam conditions in order to image all dislocations with different Burgers vectors, were used to estimate the density. Fig. 5a and b show the cross-sectional TEM images of the sample grown on the Gr/SiO_2/Si substrate. The TD

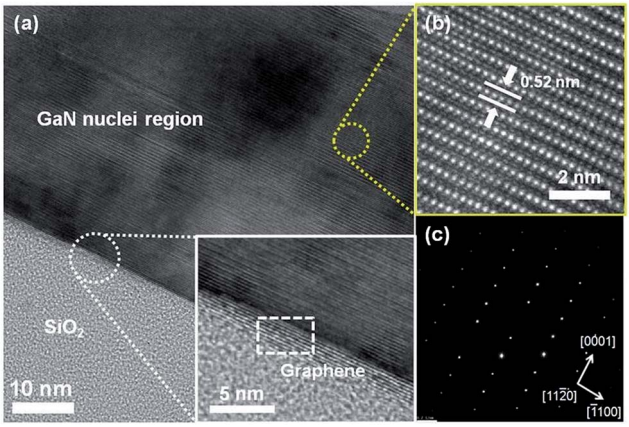

Fig. 4 (a) Low-magnification cross-sectional TEM image of GaN nuclei region on graphene. The number of graphene layers is shown in the inset image. (b) The corresponding high-resolution TEM image. (c) Electron diffraction pattern of GaN crystal grown on Gr/SiO_2/Si.

Table 3 Strain comparison of GaN on Gr/SiO_2/Si, sapphire, and Gr/sapphire. E_2^H mode phonon frequency of bulk is 567 cm^{-1} (see Kitamura *et al.*[14])[a]

	GaN on Gr/SiO_2/Si	GaN on sapphire	GaN on Gr/sapphire
$\Delta\omega$ (cm^{-1})	−1.8	+7.2	+2.7
σ_{xx} (GPa)	−0.7	+2.8	+1.1
ε (%)	0.2–0.4	0.9–1.8	0.4–0.6

[a] $\Delta\omega$ (cm^{-1}) = $C\sigma_{xx}$, $\Delta\omega$: E_2^H phonon frequency, C: linear stress coefficient (cm^{-1} per GPa) → 2.56 cm^{-1} per GPa, σ_{xx}: biaxial stress (GPa) bulk GaN → 567 cm^{-1}, E = stress/strain = σ/ε, E: Young's modulus of bulk GaN → 160–290 GPa.

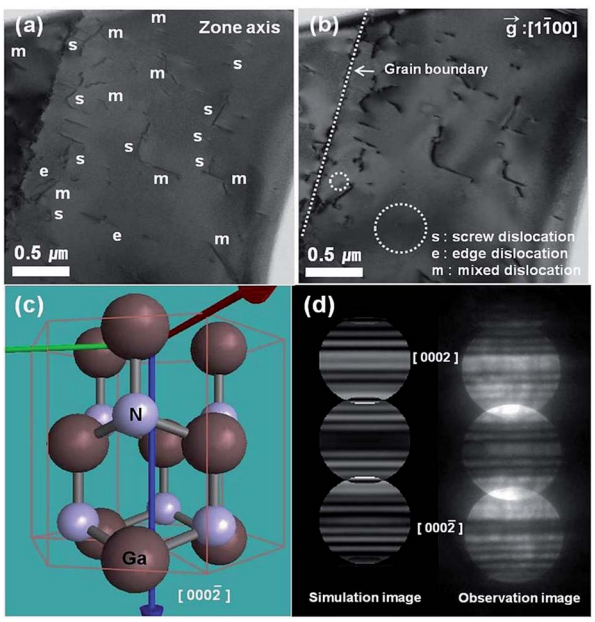

Fig. 5 Cross-sectional two-beam bright-field TEM images of GaN crystal on graphene: (a) zone axis and (b) g = [1$\bar{1}$00] image showing screw and mixed dislocations. (c) Convergent beam electron diffraction (CBED) simulation structure of stacking-grown GaN on Gr/SiO_2/Si and (d) simulated and observed CBED patterns for 160 nm thickness.

types in the GaN crystal were determined by applying the $g \cdot b$ criterion to the two-beam images of the cross-sectional TEM specimen (g is a reciprocal lattice vector and b is a Burgers vector), which were recorded near the $[11\bar{2}0]$ zone axis with $g = [1\bar{1}00]$ in Fig. 5a and b.[29]

Here we discuss pure edge dislocations in more detail. The dislocations shown only in $g = [1\bar{1}00]$ of the two-beam image are pure edge dislocations because threading dislocations have a dislocation line vector parallel to the c-axis, as shown in Fig. 5b. On the other hand, the dislocations shown in the $[11\bar{2}0]$ zone axis of the two-beam image are pure edge, pure screw, and mixed dislocations, as shown in Fig. 5a. This indicates that the predominant dislocations in GaN crystals grown on Gr/SiO_2/Si were screw- and mixed-type dislocations. The numbers of edge-, screw-, and mixed-type dislocations for GaN crystals grown on Gr/SiO_2/Si differed from those of previous studies on sapphire substrates, which revealed pure edge-type dislocations only.[30–33] The predominance of mixed-type dislocations on Gr/SiO_2/Si may be attributed to a higher density of screw-type dislocations as compared to those on GaN on sapphire. The dashed line in Fig. 5b is the grain boundary of the GaN crystal. The number of TDs was counted at random positions on a scale of 2 μm. The estimated total TD density ranged from 8×10^8 cm^{-2} to 3.6×10^9 cm^{-2}, which is comparable to that of GaN grown on sapphire, 6H–SiC, and Si(111) but slightly higher than that of GaN grown on sapphire substrates (see Table 1).

Convergent beam electron diffraction (CBED) is one of the most powerful techniques for determining the polarity of GaN crystals on graphene.[34] Since GaN is a non-centrosymmetric crystal, JEMS software was used to simulate the index of (0002) and $(000\bar{2})$ directions of the experimental patterns and consequently to deduce the nanostructure polarity (Fig. 5c and d). The intensity distribution change also depends on the sample thickness. The simulation and experimental disks agreed well with each other, indicating that these crystals were grown with Ga polarity.

Unlike typical GaN crystals grown on sapphire, GaN grown on Gr/SiO_2/Si in the current study generated edge dislocations perpendicular to the (0001) growth direction, and therefore most dislocations were buried within the GaN crystals. Thus surface etch pits were not visible on the surface of GaN grown on Gr/SiO_2/Si (Fig. 6a). Even after surface etching with 0.5 mol KOH at 80 °C for 20 min, etch pits were not visible, as shown in the two side images of Fig. 6a. On the other hand, for GaN/SiO_2/Si, several large etch pits and many small etch pits were formed, as shown in Fig. 6b. An etch pit density (EPD) of approximately 8×10^9 cm^{-2} was obtained, which is similar to the EPD of GaN grown on the sapphire substrate. The shape of the etch pits in the top view was clearly different from that of the side view, which shows cylindrical protrusions. Most dislocations were generated perpendicular to the growth direction. To demonstrate the quality of GaN crystals grown on graphene, we fabricated an light emitting diode (LED) using five-period InGaN/GaN multi-quantum wells (MQWs) (see ESI, Fig. S4†). Light emission was demonstrated from the as-fabricated LED. This opens the possibility of fabricating flexible LEDs in the near future.

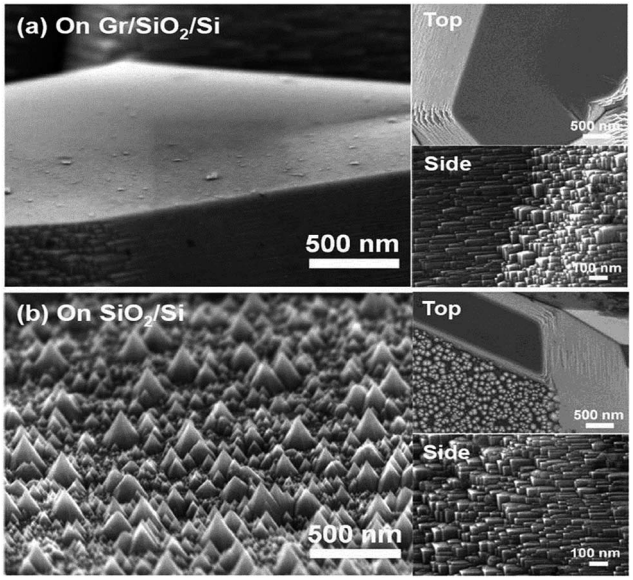

Fig. 6 FESEM images of GaN grown on (a) Gr/SiO_2/Si and (b) SiO_2/Si after etching for 20 min in 0.5 mol KOH. The right images show top and side views of GaN after etching.

Conclusion

We have grown high-quality GaN crystals directly on graphene layers without buffer layer deposition by MOCVD. The quality and microstructures of these GaN crystals revealed several unique features as compared to GaN directly grown on sapphire or SiO_2 without graphene: (i) an (0002) GaN peak perpendicular to the substrate was dominant, (ii) the GaN crystal showed mild strain, (iii) screw and screw mixed with edge dislocations were dominant, and (iv) threading dislocations were spread inside the GaN bulk and no etch pits were formed on the GaN surface. Therefore, we believe that graphene with π electrons and hexagonal symmetry could be an ideal substrate for numerous hexagonal crystal growth systems, in particular for layered structures such as BN and transition metal dichalcogenides. Further research is required to investigate the dependence of quality of crystals on the method of synthesis and the related growth parameters.

Experimental section

Preparation of graphene substrate

A 300 nm Ni film on a SiO_2 300 nm/Si substrate was prepared by electron beam (e-beam) evaporation. The growth method was similar to that described in a previous study.[11] Poly(methyl methacrylate) (PMMA) (e-beam resist, 950k C4, MicroChem) was spin coated onto the graphene/Ni film at 1000 rpm for 60 s. The sample was soaked in nickel etchant (Type I, Transene) for 3 h. After rinsing by deionized water, the PMMA/graphene layers were fished onto the SiO_2 (300 nm)/Si wafer and the PMMA was removed by acetone. Commercial atomic layer deposition (ALD) equipment (Lucida D100, NCD Technology, Korea) was used for ozone treatment at 100 °C. Ozone gas was supplied for 3 s and

purged with N_2 gas for 2 s, which comprised one cycle. This was repeated for 50 cycles.

MOCVD growth of GaN films on graphene

A GaN-based three-dimensional (3D) microstructure was grown on the graphene/SiO_2/Si substrate by metal–organic chemical vapour deposition (MOCVD, Thomas Swan). The nucleation layers were grown at 530 °C using trimethylgallium (TMGa) and ammonia (NH_3) for 5 min. The growth of a 10 μm-thick GaN-based crystal structure was performed at 1040 °C under a growth pressure of 665 mbar for 3 h. The grown GaN was etched by 0.5 mol KOH for 20 min for etch pit observations.

Characterization of graphene and GaN

The number of graphene layers was analysed using a UV-vis spectrometer and transmission electron microscope (TEM). We used the CRM 200 system (Witec, Germany) with ~20 mW of 532 nm laser for confocal Raman spectroscopy. The PL spectra were recorded in the temperature range of 10–300 K using a closed-cycle cryostat and a He–Cd laser of 325 nm excitation wavelength with a maximum input power of 15 mW. For the structural analysis, the obtained sample was measured by X-ray diffraction (XRD, Rigaku SmartLab, Japan) at a scan rate of 2 deg min^{-1} from 20 to 80 deg. To obtain cross-sectional TEM specimens of the GaN thin films a few micrometres thick, we used a conventional method.[35] The specimens were sliced into small pieces (5 mm × 2 mm). A sandwich structure was prepared by bonding two slices with the multilayers facing each other, with the glue (G-1 epoxy) on the surface of the multilayers. This sandwich structure was cured in an oven at 130 °C for up to 4 h. One side was polished to a mirror-like finish and the other side was polished by a wedge-polishing technique with a tripod polisher. After final polishing, ion milling (FISCHIONE LAMP 1010) was conducted to obtain GaN thin films. TEM observation of the GaN thin films was done by JEM 2100F (JEOL).

LED fabrication with GaN crystals on graphene/sapphire

GaN-based LEDs were grown on the graphene/sapphire substrates by MOCVD. The LED structure consisted of a Si-doped n-type GaN layer, five periods of InGaN/GaN multi-quantum wells (MQWs), and a 150 nm-thick Mg-doped p-type GaN layer. After cooling down from the thermal cleaning step, a GaN nucleation layer approximately 25 nm thick was deposited at 530 °C on the graphene/sapphire substrate. A 2 μm-thick undoped GaN epilayer was subsequently grown at 1040 °C. Thereafter, the temperature was gradually decreased to 750 °C in order to grow InGaN/GaN MQWs in N_2 ambient; the MQWs consisted of five periods of 3 nm-thick InGaN well layers and 12 nm-thick GaN barrier layers. Finally, the Mg-doped p-type GaN epilayer was grown in H_2 ambient at 950 °C (ESI, Fig. S4†).

Acknowledgements

S. J. C. and Y. H. K. contributed equally to this work. This work was supported by the Institute for Basic Science and in part by BK-Plus through Ministry of Education, Korea. This work was also supported by the Institute for Basic Science (IBS-R011-D1) in Korea.

Notes and references

1 S. Nakamura, T. Mukai and M. Senoh, *Appl. Phys. Lett.*, 1994, **64**, 1687.
2 F. A. Ponce and D. P. Bour, *Nature*, 1997, **386**, 351.
3 S. J. Rosner, E. C. Carr, M. J. Ludowise, G. Girolami and H. I. Erikson, *Appl. Phys. Lett.*, 1997, **70**, 420.
4 S. Nakamura, *Science*, 1998, **281**, 956.
5 M. F. Schubert, S. Chhajed, J. K. Kim, E. F. Schubert, D. D. Koleske, M. H. Crawford, S. R. Lee, A. J. Fischer, G. Thaler and M. A. Banas, *Appl. Phys. Lett.*, 2007, **91**, 231114.
6 Y. Gohda and S. Tsuneyuki, *Appl. Phys. Lett.*, 2012, **100**, 053111.
7 Y. J. Hong, W. H. Lee, Y. Wu, R. S. Ruoff and T. Fukui, *Nano Lett.*, 2012, **12**, 1431.
8 P. K. Mohseni, A. Behnam, J. D. Wood, C. D. English, J. W. Lyding, E. Pop and X. Li, *Nano Lett.*, 2013, **13**, 1153.
9 Y. Kim, J. Lee and G. Yi, *Appl. Phys. Lett.*, 2009, **95**, 213101.
10 H. Park, S. Chang, J. Jean, J. J. Cheng, P. T. Araujo, M. Wang, M. G. Bawendi, M. S. Dresselhaus, V. Bulovic, J. Kong and S. Gradecak, *Nano Lett.*, 2013, **13**, 233.
11 S. J. Chae, F. Güneş, K. K. Kim, E. S. Kim, G. H. Han, S. M. Kim, H. J. Shin, S. M. Yoon, J. Y. Choi, M. H. Park, C. W. Yang, D. Pribat and Y. H. Lee, *Adv. Mater.*, 2009, **21**, 2328.
12 G. H. Han, F. Gunes, J. J. Bae, E. S. Kim, S. J. Chae, H. J. Shin, J. Y. Choi, D. Pribat and Y. H. Lee, *Nano Lett.*, 2011, **11**, 4144.
13 K. Chung, C.-H. Lee and G.-C. Yi, *Science*, 2010, **330**, 655.
14 T. Kitamura, S. Nakashima, N. Nakamura, K. Furuta and H. Okumura, *Phys. Status Solidi C*, 2008, **5**, 1789.
15 D. Y. Song, M. Basavaraj, S. A. Nikishin, M. Holtz, V. Soukhoveev, A. Usikov and V. Dmitriev, *J. Appl. Phys.*, 2006, **100**, 113504.
16 W. E. Fenwick, N. Li, T. Xu, A. Melton, S. Wang, H. Yu, C. Summers, M. Jamil and I. T. Ferguson, *J. Cryst. Growth*, 2009, **311**, 4306.
17 K. Y. Zang and S. J. Chua, *Phys. Status Solidi C*, 2008, **5**, 1585.
18 D. G. Zhao, S. J. Xu, M. H. Xie and S. Y. Tong, *Appl. Phys. Lett.*, 2003, **83**, 677.
19 S. Tripathy, S. J. Chua, P. Chen and Z. L. Miao, *J. Appl. Phys.*, 2002, **92**, 3503.
20 D. Volm, K. Oettinger, T. Streibl, D. Kovalev, M. Ben-Chorin, J. Diener and B. K. Meyer, *Phys. Rev. B: Condens. Matter Mater. Phys.*, 1996, **53**, 543.
21 S. Rudin, T. L. Reinecke and B. Segall, *Phys. Rev. B: Condens. Matter Mater. Phys.*, 1990, **42**, 11218.
22 T. Ogino and M. Aoki, *Jpn. J. Appl. Phys.*, 1980, **19**, 2395.
23 R. Hirota, K. Kushida, J. Talahashi and K. Kuriyama, *Nucl. Instrum. Methods Phys. Res., Sect. B*, 2004, **219**, 792.
24 D. S. Green, U. K. Mishra and J. S. Speck, *J. Appl. Phys.*, 2004, **95**, 8456.
25 D. L. Duong, G. H. Han, S. M. Lee, F. Gunes, E. S. Kim, S. T. Kim, H. Kim, Q. H. Ta, K. P. So, S. J. Yoon, S. J. Chae,

Y. W. Jo, M. H. Park, S. H. Chae, S. C. Lim, J. Y. Choi and Y. H. Lee, *Nature*, 2012, **490**, 235.
26 T. S. Oh, Y. S. Lee, H. Jeong, J. D. Kim, T. H. Seo and E. -K. Suh, *Phys. Status Solidi C*, 2009, **2**, 589.
27 V. Narayanan, K. Lorenz, W. Kim and S. Mahajan, *Appl. Phys. Lett.*, 2001, **78**, 1544.
28 P. Vennegues, B. Beumont, M. Vaille and P. Gibart, *J. Cryst. Growth*, 1997, **173**, 249.
29 P. B. Hirsch, A. Howie, R. B. Nicholson, D. W. Pashley and M. J. Whelan, in *Electron Microscopy of Thin Crystals*, Krieger, New York, 1977.
30 X. H. Wu, L. M. Brown, D. Kapolnek, S. Keller, B. Keller, S. P. DenBaars and J. S. Speck, *J. Appl. Phys.*, 1996, **80**, 3228.
31 D. Kapolnek, X. H. Wu, B. Heying, S. Keller, B. P. Keller, U. K. Mishra, S. P. Denbaars and J. S. Speck, *Appl. Phys. Lett.*, 1995, **67**, 1541.
32 J. L. Rouviere, M. Arlery, B. Daudin, G. Feuillet and O. Briot, *Mater. Sci. Eng., B*, 1997, **50**, 61.
33 W. Qian, M. Skowronski, M. Degraef, K. Doverspike, L. B. Rowland and D. K. Gaskill, *Appl. Phys. Lett.*, 1995, **66**, 1252.
34 H. Morkoc, *Mater. Sci. Eng., R*, 2001, **33**, 135.
35 J. Chen and D. G. Ivey, *Micron*, 2002, **33**, 489.
36 G. Popovici, G. Y. Xu, A. Botchkarev, W. Kim, H. Tang, A. Salvador, H. Morkoc, R. Strange and J. O. White, *J. Appl. Phys.*, 1997, **82**, 4020.
37 K. Lee, B. L. VanMil, M. Luo, L. Wang, N. C. Giles and T. H. Myers, *Phys. Status Solidi C*, 2005, **2**, 2204.
38 W. Gotz, N. M. Johnson, C. Chen, H. Liu, C. Kuo and W. Imler, *Appl. Phys. Lett.*, 1996, **68**, 3144.
39 A. Zado, E. Tschumak, J. W. Gerlach, K. Lischka and D. J. As, *J. Cryst. Growth*, 2011, **323**, 88.